

Participation of Load Resources in Day-ahead Market to Provide Primary-Frequency Response Reserve

Cong Liu, *Senior Member, IEEE*, Pengwei Du, *Senior Member, IEEE*

Abstract —With integration of more and more renewable energy resources, it is becoming increasingly difficult to maintain adequate primary frequency control (PFC) capability for a future power grid, especially under low system inertia conditions. Load resources (LRs) equipped with under-frequency relays can participate in PFC supplementing to the governor responses from synchronous units. In this paper, we propose an energy, inertia and frequency response reserve (FRR) co-optimization formulation in the day-ahead market where both primary frequency reserve (PFR) from synchronous generators and fast frequency response reserve (FFR) from LRs are procured in a cooperative way to meet the desired FRR need tied to the system inertia condition. Since FFR is more effective than PFR in arresting the frequency decline, the proposed approach will yield different marginal prices for FFR and its PFR counterpart to award the speed of response. As the formulation proposed involves bilinear terms in optimization problem, a linear reformulation techniques with big M is proposed to transform the problem into a mixed integer linear programming which can be solved by the commercial solver CPLEX. The case study shows the effectiveness of the proposed approach and the correctness of the quantities and prices of the cleared reserve.

Index Terms—frequency response reserve, unit commitment, reserve, co-optimization, dynamic simulation.

I. NOMENCLATURE

Indexes:

i	Index of generating units
j	Index of loads
t	Index of time periods
s	Index of segments
q	Index of segment in stepwise start-up curves
l	Index of transmission branches

Variables:

P	Cleared energy
L	Cleared demand
I, Y, Z	Binary indicators for unit on/off, start-up and shutdown
δ	Binary variables indicating a segment in a linearized curve is activated
STC	Start up cost of a generating unit
RUP	Regulation up reserve of generating units
RDN	Regulation down reserve of generating units
NSR	Non-spinning reserve of generating units
PFR	Cleared frequency response reserve from primary frequency response of generating units

FFR	Cleared frequency response reserve from fast frequency response of loads
FRR	Total cleared frequency response reserve
$RUPN$	Not served regulation up reserve
RDN	Not served regulation down reserve
$FRRN$	Not served frequency response reserve
$NSRN$	Not served non-spinning reserve
$PFRN$	Not served primary frequency response reserve
Inx	Inertia value of a segment in a linearized curve
β	Variables to replace bilinear terms
$\lambda, \theta, \gamma, \rho, \tau, \pi, \sigma$	Shadow prices

Functions:

α	Equivalent Ratio between FFR and PFR, depending on the total inertias of committed generation units
$Rfrr$	Total requirement of frequency response reserve, depending on the total inertias of committed generation units
Ce	Energy cost/benefit curve based on energy offers/bids

Constant and Sets:

G	Set of generating units
D	Set of demands
T	Set of time periods
B	Set of transmission branches
N	Set of segments
Csu	Step constant in the start-up cost curve of a generating unit
Cf	Minimum energy price
$Crudn, Crup$	Offer price for regulation up and down reserve from generating units
$Cffr, Cnsr$	Offer price for fast frequency response from loads and non-spinning reserve from generating units
$Cpfr$	Offer price for primary frequency response reserve from generating units
$Nrup, Nrdn$	Penalty price for unserved regulation up and down
$Nfrr, Nnsr$	Penalty price for unserved frequency responsive reserve and non-spinning reserve
$Npfr$	Penalty price for unserved primary frequency response reserve from generating units
$Rrup, Rrdn$	Total requirement of regulation up/down reserve
$Rnsr$	Total requirement of frequency responsive reserve and non-spinning reserve

C. Liu and P. Du are with Electric Reliability Council of Texas, Taylor, TX 76574, United States of America. E-mails: cong.liu@ercot.com and pengwei.du@ercot.com.

$Rpfr$	Total requirement primary frequency response reserve from generating units
LSL, HSL	Low and high sustainable limits of generating units
MPC	Maximum power consumption for a demand
MT_{on}, MT_{off}	Minimum on/off time of generating units
RU, RD	Maximal ramp up/down limits per hour of generating units
QSC	Quick start capacity of generating units in 30 minutes
H	Inertial constant
S	Rated power of generating units
SF	Generator/load shift factor of power network
\overline{PL}	Capacity limit of a transmission branch
$\overline{RUP}, \overline{RDN}, \overline{PFR}$	Upper bounds of available regulation up/down reserves and PFR of generating units
$Ratio$	The step value of the Ratio-Inertia curve
$RFRR$	The point value in vertical scale of the FRR requirement-Inertia curve
In	The inertia value of the linearized curves
M	A larger positive number

II. INTRODUCTION

Maintaining system frequency at its target value is critical for power grid operation [1]. Future power systems will see significant growths of renewable generation resources (RGSs) and their impact on the frequency control has been recently investigated [2-5]. In North America, the overall task of controlling frequency is organized in three levels, namely, the primary, secondary and tertiary frequency control. Among these three levels, the primary frequency control is of particular importance as more synchronous machines could be displaced from dispatch by RGSs. In [6-9], the authors demonstrated that the large-scale integration of RGSs leads to decline in system inertia¹, causing a significant reduction of the primary frequency control (PFC) capability. Electric grids in North America also have witnessed this deterioration in the PFC capability over the past decades. Similar studies conducted for the Ireland grid also show that if no grid enhancement is implemented soon, the risk of constraining or curtailing a significant amount of wind generation would be very high because of the lack of adequate PFC [10-11]. Therefore, whether or not those low-inertia power systems can procure and maintain adequate frequency response reserve (FRR) for providing PFC to respond to credible large contingencies is becoming a serious concern.

The Electric Reliability Council of Texas (ERCOT) is an Independent System Operator (ISO) serving over 23 million customers in Texas. As a single Balancing Authority (BA) without synchronous connections to its neighboring systems, ERCOT relies purely on its internal resources to balance power shortages and variations. As more than 25 GW wind generation capacity will be added to the ERCOT grid by 2020 [33], it is anticipated that a large volume of FRR will be required. In

addition to reliability concerns, the procurement of FRR is also very costly. For example, ERCOT spends more than 100 million U.S. dollars annually on procuring FRR [34].

Alternative resources have been suggested for providing FRR, such as synthetic inertia from wind turbines [12], energy storages [13], and fast-acting load resources (LRs). Fast-acting LRs are specially a promising technology as they can quickly stabilize the frequency for the losses of large generation units while their cost in provision of FRR is relatively low. However, how to coordinate the governor responses and LRs in a concert to meet the desired reliability need is still a question, especially in a market context.

Recent works more focus on a market design incorporating primary frequency reserve mechanism to incentivize synchronous generators to provide PFC [14-21]. The basic principle of scheduling and pricing of coupled energy and primary, secondary, and tertiary reserves is discussed in [14]. A simplified dynamic model is introduced to determine the minimum spinning reserve requirement that is used as part of the constraints in economic dispatch for a pool-based power market [15-17]. The dependency between the system inertia and the need of FRR is approximately taken into account in the scheduling process [18]. More detailed models of the governor responses are adopted in [19-20] to calculate the pricing of FRR influenced by different dynamic characteristics of the governors. The problem formulation of accounting for FRR constraints in unit commitment is described in [21]. Those studies focused primarily on the provision of primary frequency response from synchronous generators without considering other viable resources.

The most recent work at ERCOT evaluated the efficiency of LRs² relative to synchronous machines in providing FRR, and a new framework was developed to allow both LRs and synchronous machines to bid in the real-time FRR market with the commitment status of generators fixed [22]. As the FRR need is determined a priori, the proposed approach is formulated as a security constrained economic dispatch (SCED) problem augmented with an added FRR constraint.

In this paper, we propose a day-ahead energy, inertia and reserve co-optimization formulation in which the FRR requirement can be met by both primary frequency reserve (PFR) from synchronous generators and fast response reserve (FFR) from load. The work reported in this paper is an extension of the previous work in [22], which is limited to the real-time market, but is formulated as a nonlinear programming optimization problem. Compared to [22], this work can explicitly consider the inter-dependency between the commitment decision, inertia and PFR/FFR so that it essentially solves a unit commitment (UC) problem. Unlike the study in [31], the work conducted here determines the award of FFR in the framework of the unit commitment while it does not require the dynamic simulation as part of the optimization problem, which makes the problem more tractable. By doing this, this approach is also scalable for a large-sized grid.

In summary, this paper solves a practical, efficient and scalable unit commitment where inertia, PFR and FFR are co-

¹ Inertial is a property of large synchronous generators, which contain large synchronous rotating masses, and which acts to overcome the immediate imbalance between power supply and demand for electric power systems.

² These are industrial loads operated on schedule.

optimized with energy. The contributions of this papers are summarized as follows.

1) The need of PFR and FFR is determined based on the system inertia, which can be impacted by how synchronous generating units are committed. This constraint is considered in the unit commitment problem as a nonlinear function of inertia and reserve requirement determined from dynamic studies.

2) An equivalency ratio between PFR and FFR is used to account for their difference in the efficiency in arresting the frequency deviations. An empirically-determined nonlinear function of inertia and ratio based on dynamic studies is included in the proposed formulation. This pay-for-performance design will lead to a more efficient market operation and produce a proper incentive price signal to fast-acting resources.

3) This paper consider a mixed integer bilinear model where the decision variables include unit commitments (inertia), reserve requirements, equivalent ratio, and cleared reserves. The linear reformulation techniques are proposed with big M to transform it into a mixed integer linear programming which can be solved by the commercial solver CPLEX. A warm start technique is proposed to accelerate the computational speed.

The rest of this paper has the following structure. Section III introduces frequency response reserve at ERCOT. Section IV presents quantification of FRR requirement at ERCOT. Section IV focuses on the mathematical model of co-optimization engine. Section V contains case studies, while conclusions are provided in Section VI.

III. FREQUENCY RESPONSE RESERVES AT ERCOT

In ERCOT, the FRR service is divided into two categories, i.e., PFR provided by synchronous generators and FFR provided by other resources (e.g. fast response loads, energy storage systems).

PFR is provided by online synchronous generators through governor response or governor-like actions to arrest and/or counter-respond to frequency deviations. As a single BA, ERCOT must comply with the BAL-003 standard [30]. The frequency response obligation (FRO) for ERCOT is 413MW/0.1Hz. To meet this requirement, ERCOT requires every resource with a speed governor to put the governor in service whenever the resource is online. In addition, the droop setting should not exceed 5% and the frequency response dead band should be no more than ± 0.017 Hz.

FFR is a response from a resource that is self-deployed to provide a full response within 30 cycles after frequency meets or drops below certain threshold. To provide FFR, a load resource will be equipped with an under-frequency relay (e.g. triggered if the frequency is dropped under 59.7 Hz). As required by ERCOT, the response time of FFR should be less than 500 ms (including the frequency relay pickup delay and the breaker action time). This makes FFR more effective to mitigate the decline of the frequency compared to the PFR because a generator providing PFR needs seconds to react to the change in the frequency. Therefore, the deployment of FFR will allow PFR resources more time to respond to large frequency changes. It is also able to improve the frequency nadir and be instrumental in preventing frequency from

dropping below the involuntary under-frequency load shedding (UFLS) threshold when losing large generation units.

IV. MINIMUM FRR REQUIREMENT

A sufficient amount of FRR should be carried so that the power system can withstand the simultaneous losses of two largest generation units. At ERCOT, the minimum requirement for the quantities of FRR is determined based on the following reliability criterion: for contingencies such as the losses of two largest units (2750 MW), the system frequency should be arrested before triggering UFLS and the frequency nadir should be maintained above 59.3 Hz.

Traditionally, the minimum FRR requirement is derived based on a single worst-case scenario where the load is low and the wind generation is high. Following this approach, a minimum of 2800 MW FRR was required for every hour in a year at ERCOT prior to the year of 2016 [9]. However, integrating large amounts of renewable generation resources has caused a noticeable decline in the system inertia. In addition, the system inertia could vary largely across a year. Using a worst-case scenario to determine the FRR need becomes either inefficient (e.g. over-procure FRR at high-inertia hours) or inadequate (e.g. under-procure FRR at low-inertia hours).

A recent study has examined how much FRR is needed with a direct linkage to the system inertia condition and also investigated how to coordinate PFR and FFR to meet the system need [22]. In this study, a total 12 representative cases from ERCOT historical operations with an inertia between 120 GW·s and 350 GW·s were selected to cover the spectrum of the system inertia levels. Table I summarizes the results of all 12 cases. It shows that the minimum FRR requirement, $Rfrr_t$, increases as the inertia decreases.

The FRR constraint should be satisfied as follows

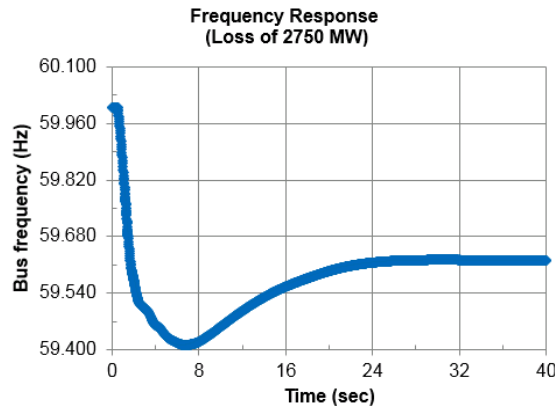
$$FRR_t = \sum_{i \in G} PFR_{i,t} + \alpha_t \cdot (\sum_{j \in D} FFR_{j,t}) \geq Rfrr_t \quad (1)$$

To fulfill ERCOT's frequency response obligation in BAL-003 standard [30] (413MW/0.1Hz), a minimum amount of PFR, $Rpfr_t$ (1150 MW), need to be provided by generators as

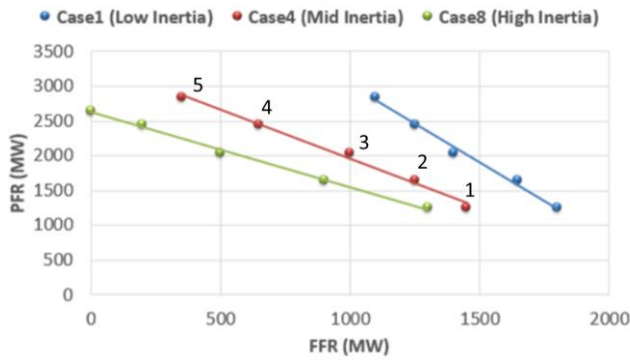
$$\sum_{i \in G} PFR_{i,t} \geq Rpfr_t \quad (2)$$

The concept of the equivalency ratio, α_t , was introduced as the performance metric for FFR and allows PFR to be substituted by FFR without compromising the system PFC capability. This equivalency ratio can be interpreted as: 1 MW of FFR is 2.2 times as effective as 1 MW of PFR in arresting the frequency decline when the system inertia condition is at 120 GW·s, i.e., each 1 MW of FFR can be replaced by 2.2 MW of PFR.

This equivalency ratio α_t , is calculated from dynamics simulation. In the simulation, the minimum requirement of PFR and FFR for a given inertia condition can be identified when the lowest frequency dip equals to 59.4 Hz after two largest units (2750 MW) are tripped – see Fig. 1 (a). One example of different combinations of PFR and FFR requirement is shown in Fig. 1 (b) for the low, medium, and high inertia conditions. The approximately linear slope of these curves are then derived as an equivalency ratio α_t between PFR and FFR requirements. More details can be found in [22].



(a) Simulated frequency response at minimum PFR and FFR



(b) Combinations of minimum PFR and FFR requirements at low, medium, and high system inertia conditions

Fig. 1. Illustration of deriving minimum PFR/FFR requirement and equivalent ratio

The value of α_t is greater than 1.0 when the system inertia is less than 297 GW·s as shown in Table I. It means that FFR is more effective than PFR when stabilizing the frequency at low inertia conditions (e.g. Cases 1 through 8). However, the effectiveness decreases when the system inertia increases. When inertia is higher than 297 GW·s, FFR and PFR becomes equally effective. This is because there are more generators online under heavy loading conditions so that the overall system inertia is higher, making the rate of changing the frequency following the disturbance much less than that in a low-inertia condition. As a result, the aggregated slow-acting governor-like response has enough time to react to the loss of generation. The results also demonstrate that fast load response is more valuable in arresting the frequency drops when response speed is more critical, which is the case in low-inertia systems.

TABLE I. MINIMUM FFR REQUIREMENT AND EQUIVALENCY RATIOS

Case No.	Inertia (GW·s)	$Rfrr_t$ (MW)	Equivalency Ratio (α_t)
1	120	5200	2.2
2	136	4700	2.0
3	152	3750	1.5
4	177	3370	1.4
5	202	3100	1.3
6	230	3040	1.25
7	256	2640	1.13
8	278	2640	1.08

9	297	2240	1
10	316	2280	1
11	332	2140	1
12	350	2140	1

V. CO-OPTIMIZATION OF ENERGY AND RESERVE

A. Day-ahead market co-optimization model

The day-ahead market energy and reserve co-optimization problem is a security-constrained unit commitment problem. The objective function is to maximize the social welfare which is the sum of demand benefits based on demand bids minus energy costs based on generators' three part offers, reserve costs based on reserve offers from both generating units and demands and unserved reserve cost based on penalty prices as shown in (3). The start-up cost is a function of the number of hours the generator has been turned off. The constraint (4) implicitly determines the start-up costs of generating units in each hour during the optimization process. q represents the index of time segments in stepwise start-up curves. STC_{it} will be zero resulted from the optimization process if the unit does not change its status from off to on at hour t .

Formulations (5)–(8) represent unit commitment status and coupling constraints. If the binary unit variable is 1, the unit status is on. Otherwise, it is off. The start-up and shut-down indicators are relaxed in this study to become continuous variables in (8) in order to accelerate the computational speed of solving the mixed integer programming problem by using the branch and cut strategy [29]. Formulations (5)–(7) will restrict these continuous variables to be binary value based on binary unit statuses. Formulation (9)–(11) represent the operational characteristics of individual thermal units, such as ramp rate and minimum on/off time [24]–[26]. Ramp rate limits restrict the change of power production in two adjacent hours. Minimum on/off time represents that the generator has to stay online/offline for the required period of time before it is turned off/on again. Formulation (9) and (10) state that if a unit is in start-up or shut-down in the past minimum on/off time, the unit status in current hour has to be on/off. Constraint (12)–(16) defines the bounds for the generations and the reserves for each unit. Only the unit that is offline and has quick start capability within 30 minutes can provide non-spinning reserve as shown in (17). Constraint (18) shows that the frequency response reserve from a load resource must be less than its maximum power consumption that is the highest point in its bid curve. The essential scheduling problem in day-ahead market is to balance cleared energy supply with demand, so hourly generation and cleared demand must satisfy the power balance constraint (19). Constraint (20) represents transmission constraints under normal or contingency condition. Usually, the network security check is separated from unit commitment problem. Only activated transmission constraints will be added into security-constrained unit commitment constraints. Shift factors in (20) represent a measure of how the flow on a particular transmission element is changed due to a unit injection of power from a particular Electrical Bus to a fixed reference Electrical Bus. Constraint (21)–(24) denotes the traditional regulation up/down and non-spinning reserve requirement constraints in system wide. The non-served reserve is penalized into the objective function, which can be equivalent to introducing a steep reserve

demand curve. The penalty prices for non-served reserve are usually high so that reserve will be bought in normal condition.

The minimum requirement of PFR is given in formulation (25), which implies that at least some synchronous generating units should be committed to contribute their inertias to the system. Compared with (2), non-served reserve $PFRN$ in (25) is introduced to ensure the optimization problem is always feasible. The equivalent ratio α_t in (1) and (27) is a measure of FFR performance so that FFR can be equivalently substituted by PFR without sacrificing the performance of PFC capability. Equation (1) and (27) indicates that the FFR requirement can be determined by the overall FFR need, the equivalency ratio as well as the amount of PFR. As indicated in Table I, the overall FFR requirement $Rfrr_t$ and the equivalent ratio α_t in (1) is a function of the system inertia. Because the system inertia accounts for the inertia of each individual generating unit if it is committed and synchronized online, each unit commitment status implicitly depends on $Rfrr_t$ and α_t in (26)-(27). Compared with (1), non-served reserve $FRRN$ in the constraint (26)-(27) is introduced to ensure the optimization problem is always feasible. However, the penalty price for $FRRN$ is normally high to penalize a shortage in the PFC capacity if it exists. FFR requirement-Inertia and Ratio-Inertia relationship and in (26)-(27) are a nonlinear function and formulation (27) includes bilinear terms which is product of two variables so that the model (3)-(27) is a mixed integer nonlinear programming which is not effectively solved via commercial solvers, in a reasonable computational time, especially when applied to large-scale power systems. In the next section, we will show how to linearize the FFR requirement-Inertia and the Ratio-Inertia curves and transform bilinear terms by using the linear formulation with big M constraints. In this way, the mixed integer nonlinear programming model can be reformulated into a mixed integer linear or quadratic programming model.

$$\begin{aligned}
 \text{Max} \quad & \sum_{j \in L} \sum_{t \in T} [C e_{j,t}(L_{j,t}) - C f f r_{j,t} \cdot FFR_{j,t}] \\
 & - \sum_{i \in G} \sum_{t \in T} [STC_{it} + C f_i \cdot I_{i,t} \cdot LSL_i + C e_{i,t}(P_{i,t}) \\
 & \quad + C r u p_{i,t} \cdot RUP_{i,t} + C r d n_{i,t} \cdot RDN_{i,t} \\
 & \quad + C n s r_{i,t} \cdot NSR_{i,t} + C p f r_{i,t} \cdot PFR_{i,t}] \\
 & - \sum_{t \in T} [N r u p_t \cdot RUPN_t + N r d n_t \cdot RDNN_t \\
 & \quad + N n s r_t \cdot NSRN_t + N p f r_t \cdot PFRN_t \\
 & \quad + N f r r_t \cdot FRRN_t]
 \end{aligned} \tag{3}$$

s.t.

$$STC_{it} \geq C s u_{i,qc} \cdot \left[Y_{i,t} - \sum_{n=1}^{\min(t,q)} I_{i,t-n} \right], STC_{it} \geq 0 \quad \forall i \in G, t \in T \tag{4}$$

$$1 - I_{i,t-1} \geq Y_{i,t} \quad \forall i \in G, t \in T \tag{5}$$

$$I_{i,t-1} \geq Z_{i,t} \quad \forall i \in G, t \in T \tag{6}$$

$$I_{i,t} - I_{i,t-1} = Y_{i,t} - Z_{i,t} \quad \forall i \in G, t \in T \tag{7}$$

$$0 \leq Y_{i,t}, Z_{i,t} \leq 1, I_{i,t} \in \{0,1\} \quad \forall i \in G, t \in T \tag{8}$$

$$I_{i,t} \geq \sum_{\tau=\max\{1,t-MT_{on,i}+1\}}^t Y_{i,\tau} \quad \forall i \in G, t \in T \tag{9}$$

$$1 - I_{i,t} \geq \sum_{\tau=\max\{1,t-MT_{off,i}+1\}}^t Z_{i,\tau} \quad \forall i \in G, t \in T \tag{10}$$

$$-RD_i \leq P_{i,t} - P_{i,t-1} \leq RU_i \quad \forall i \in G, t \in T \tag{11}$$

$$P_{i,t} + RUP_{i,t} + PFR_{i,t} \leq HSL_i \cdot I_{i,t} \quad \forall i \in G, t \in T \tag{12}$$

$$P_{i,t} - RDN_{i,t} \geq LSL_i \cdot I_{i,t} \quad \forall i \in G, t \in T \tag{13}$$

$$0 \leq RUP_{i,t} \leq \overline{RUP}_i \cdot I_{i,t} \quad \forall i \in G, t \in T \tag{14}$$

$$0 \leq RDN_{i,t} \leq \overline{RDN}_i \cdot I_{i,t} \quad \forall i \in G, t \in T \tag{15}$$

$$0 \leq PFR_{i,t} \leq \overline{PFR}_i \cdot I_{i,t} \quad \forall i \in G, t \in T \tag{16}$$

$$0 \leq NSR_{i,t} \leq QSC_i \cdot (1 - I_{i,t}) \quad \forall i \in G, t \in T \tag{17}$$

$$0 \leq FFR_{j,t} \leq L_{j,t} \leq MPC_{j,t} \quad \forall j \in D, t \in T \tag{18}$$

$$\sum_{i \in G} P_{i,t} = \sum_j L_{d,t} \quad \forall t \in T \tag{19}$$

$$-\overline{PL}_l \leq \sum_{i \in G} SF_{l,i} P_{i,t} + \sum_{j \in L} SF_{l,j} L_{j,t} \leq \overline{PL}_l \quad \forall l \in B, t \in T \tag{20}$$

$$RUPN_t, RDNN_t, NSRN_t, NPFR_t, FRRN_t \geq 0 \tag{21}$$

$$RUPN_t + \sum_{i \in G} RUP_{i,t} \geq Rrup_t \quad \forall t \in T \tag{22}$$

$$RDNN_t + \sum_{i \in G} RDN_{i,t} \geq Rrdn_t \quad \forall t \in T \tag{23}$$

$$NSRN_t + \sum_{i \in G} NSR_{i,t} \geq Rnsr_t \quad \forall t \in T \tag{24}$$

$$PFRN_t + \sum_{i \in G} PFR_{i,t} \geq Rpfrr_t \quad \forall t \in T \tag{25}$$

$$FRRN_t + FRR_t \geq Rfrr_t (\sum_{i \in G} I_{i,t} \cdot H_i \cdot S_i) \quad \forall t \in T \tag{26}$$

$$FFR_t = \sum_{i \in G} PFR_{i,t} + \alpha_t (\sum_{i \in G} I_{i,t} \cdot H_i \cdot S_i) \cdot (\sum_{j \in D} FFR_{j,t}) \quad \forall t \in T \tag{27}$$

B. Solution of day-ahead market co-optimization

Discrete points in the FFR requirement-Inertia curve and the Ratio-Inertia curve are obtained from dynamic simulation as shown in Table I of Section IV. In this paper, we approximate the Ratio-Inertia and the FFR requirement-Inertia relationships by using stepwise linear curve and piecewise linear curve as displayed in the Fig. 2 and Fig. 3.

In order to represent linearized curves in optimization model, formulation (26)-(27) are reformulated by (28)-(32). We introduce additional binary variables to represent activation of a segment in piecewise linear and stepwise curves. The constraint (32) denotes that the current segment must be activated if the next segment is activated. Formulation (31) defines the upper bound and the lower bound of inertia value of a segment. If the next segment is activated, the current segment must be binding to its maximum value. If the current segment is not activated, the current segment must be equal to zero. Equation (30) represents that the total system inertia is equal to the summation of the inertia value of all segments. The FFR requirement for each delivery hour $Rfrr_t$ is equivalent to the right hand side of (29) where IR_s represents the slope of a segment in a piecewise linear curve. The stepwise ratio curve can be represented by the bilinear terms which are the products of the binary variables corresponding every segments and the continuous variables of cleared FFR as shown in (28).

$$FRR_t = \sum_{i \in G} PFR_{i,t} + [\sum_{s \in N} Ratio_s \cdot (\delta_{s,t} - \delta_{s+1,t})] \cdot (\sum_{j \in D} FFR_{j,t}) \quad \forall t \in T \quad (28)$$

$$FRR_t + FRR_t \geq RFRR_1 + \sum_{s \in N} IR_s \cdot In_{s,t} \quad \forall t \in T \quad (29)$$

$$In_1 + \sum_{s \in N} In_{s,t} = \sum_{i \in G} I_{i,t} \cdot H_i \cdot S_i \quad \forall t \in T \quad (30)$$

$$(In_{s+1} - In_s) \cdot \delta_{s+1,t} \leq In_{s,t} \leq (In_{s+1} - In_s) \cdot \delta_{s,t} \quad \forall s \in N, t \in T \quad (31)$$

$$\delta_{s,t} \geq \delta_{s+1,t}, \delta_{s,t} \in \{0,1\} \quad \forall s \in N, t \in T \quad (32)$$

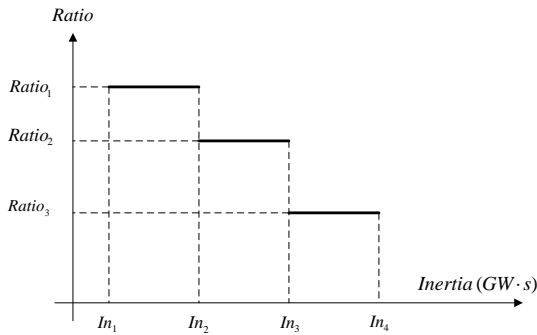


Fig. 2. Stepwise ratio-Inertia curve

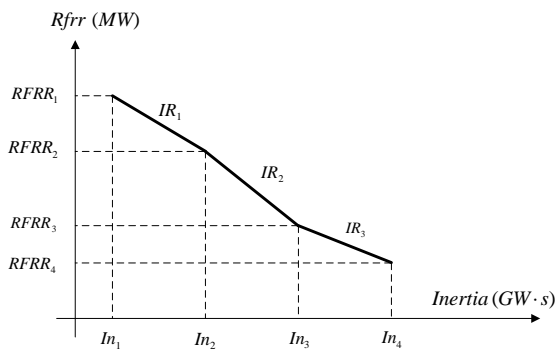


Fig. 3. Piecewise linear FRR requirement-Inertia curve

However, due to the bilinear terms, the optimization model (3)-(25) and (28)-(32) still cannot be solved by commercial solvers effectively. The way to solve this problem is to expand the feasible region by the big M method. We reformulate the bilinear terms in (28) by using some linear big M constraints as described in (33)-(35). If the binary variables $\delta_{s,t} - \delta_{s+1,t}$ is equal to zero, the constraints (34)-(35) are relaxed due to the big M constant. Otherwise, β_t is binding to the linear term, $Ratio_s \cdot \sum_{j \in D} FFR_{j,t}$. Therefore (33)-(35) is equivalent to (28). For bilinear item, if one of the variables is binary, then it can be linearized using alternative method without losing tightness as shown in [35]. On the other hand, as this methods introduces more decision variables, it might cause a computational issue. The choice of the big M value is crucial to the computational speed of branch and cuts process to solve the proposed mixed integer linear programming model (3)-(25) and (29)-(35). Setting big M too small can lead to infeasible or suboptimal solutions. Therefore, the value of big M will typically have to be rather large in order to exceed the largest activity level. When big M is large, the solver may discover that the feasible region of continues relaxation of the integer programming problem is also large. It can increase upper bound of the mixed integer programming (MIP) (if the objective is to maximize the

social welfare) to a significant level and thereby the MIP gap is hardly reduced. In order to make the problem tighter, the value of big M should be as small as possible and exceed the largest activity level. Therefore, we chose $M_{s,t} = Ratio_s \cdot \sum_{j \in D} MPC_{j,t}$ in this paper to make the problem tighter. In practice, since only a portion of load resources may provide FFR, we can reduce the big M to a reasonably small value.

$$FRR_t = \sum_{i \in G} PFR_{i,t} + \beta_t \quad \forall t \in T \quad (33)$$

$$\beta_t \geq Ratio_s \cdot \sum_{j \in D} FFR_{j,t} - M_{s,t} \cdot (1 - \delta_{s,t} + \delta_{s+1,t}) \quad \forall s \in N, t \in D \quad (34)$$

$$\beta_t \leq Ratio_s \cdot \sum_{j \in D} FFR_{j,t} + M_{s,t} \cdot (1 - \delta_{s,t} + \delta_{s+1,t}) \quad \forall s \in N, t \in D \quad (35)$$

C. Clearing prices

Given the fixed unit commitment statuses resulted from solving the day-ahead energy and reserve co-optimization problem (3)-(25) and (29)-(35), $Rfrr_t$ and α_t are determined. The mixed integer nonlinear programming model (3)-(27) become a linear programming or quadratic programming model which is used for the pricing run to obtain the clearing prices for energy and reserves.

Assume that the dual variables $\lambda, \theta, \gamma, \rho, \tau, \pi, \sigma$ are corresponding to the constraints (20)-(26) in the pricing run respectively with the fixed unit commitment statuses, $Rfrr_t$ and α_t . The locational marginal price for the energy is calculated by $\lambda_t - \sum_{l \in B} SF_{l,bus} \cdot \theta_l$. The prices for regulation up/down and non-spinning reserves are γ, ρ, τ respectively. The shadow price for PFR is π for meeting the minimum PFR requirement (25) and σ for meeting the minimum FRR requirements (26), so the price for PFR is $\pi + \sigma$. The FFR price is $\alpha_t \cdot \sigma$ to account for the equivalency ratio between the FFR and PFR.

Once the unit commitment status is given, the system inertia is fixed. Since the variable of the nonlinear empirical functions is the system inertia, the non-convexities are then essentially caused by unit commitment problem itself. In order to overcome the revenue shortages of generators, uplift payments or the new pricing strategies can be used in the settlement. For example, extended shadow prices obtained by relaxing the unit commitment binary variables in a pricing run, can generate price signals which may compensate the partial fixed costs and start-up costs of generators and the other costs caused the new introduced non-convexity [36]. This will be part of our future work as suggested.

VI. CASE STUDIES

All algorithms are implemented in AMPL and solved with CPLEX 12.5. The test environment is AIX server with four 4.024-GHz CPU processors and 64 GB of RAM. The MIP gap is set as 0.6%.

The computational study is based on the modified IEEE-118 bus system [21]. The modified IEEE-118 bus power system consists of 54 thermal generating units, 118 buses, and 186 transmission lines. The total installed capacity of 54 thermal generating units is scaled up to 60,000 MW installed thermal generation capacity at ERCOT. The susceptances and thermal rates of transmission branches are also increased in proportion. In this paper, we focus on the modeling of energy and reserve

schedule problem with considering high penetration of renewables. Six identical wind farms are added to bus 11, 15, 54, 59, 80 and 90. It is assumed that all wind power offers are \$0.01/MWh. The inertia constant of generating units are given in Fig. 4. The inertia of a generation unit equals to the inertia constant multiplied by its MVA rating. When a unit is online, it can provide its full inertia regardless of its power output. The maximum capacity for the regulation up reserve, the regulation down reserve and the PFR reserve of generating units are set as 5%, 5% and 20% of their high sustainable limit (HSL). The offer prices of the regulation up reserve, the regulation down reserve, the non-spinning reserve and the PFR reserve are set as 33.3%, 33.3%, 10% and 20% of the prices of their first energy offer segment. The regulation up/down and non-spinning reserve requirements for different hours in March 2017 can be found in the public market information website of ERCOT [32]. The minimum PFR requirement and FFR requirement are related to the system inertia, which are listed in Table I.

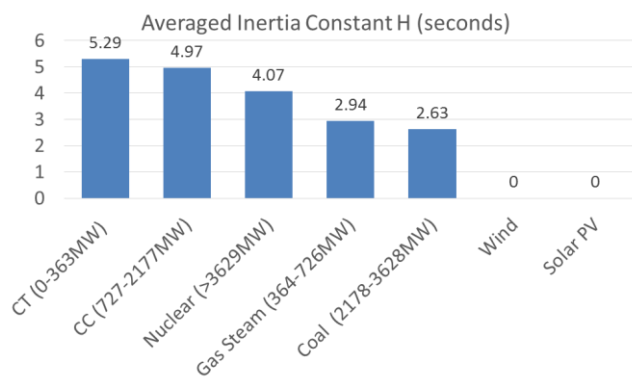


Fig. 4. Inertia constant of different generating units

We assume that there are three load resources in the day-ahead market. The peak capacity of the load resources are listed in Table II at hour 19. The load resources are elastic load with bidding prices \$90/MWh, \$35/MWh and \$6/MWh. The percentage of the capacities of the load resources at different hours are listed in Table III. We assume that all load resources at different hours have the same bidding prices and FFR offer prices.

TABLE II. BIDDING PARAMETERS AND CAPACITIES OF LOAD RESOURCES

Hour 19 (Peak)	Load capacity (MW)	Load bid (\$/MWh)	FFR offer (\$/MW)
L1	29406	90	45
L2	8822	35	5
L3	2941	6	3

TABLE III. CAPACITY PERCENTAGES OF LOAD RESOURCES

Hour	Load capacity percentage	Hour	Load capacity percentage	Hour	Load capacity percentage
1	79%	9	76%	17	86%
2	75%	10	79%	18	99%
3	72%	11	81%	19	100%
4	71%	12	83%	20	98%
5	71%	13	84%	21	96%
6	72%	14	84%	22	92%
7	74%	15	83%	23	86%

8	75%	16	82%	24	80%
---	-----	----	-----	----	-----

Three scenarios are simulated, which are described as follow.

Case A - Low penetration of wind generation and low offer prices of FFR. The peak wind-power generation in this base case is 3598 MW at hour 4 so that the wind-power penetration is about 13% at that hour. The hourly maximum wind generation profiles are shown in Table IV. The FFR offers of load resources are given in Table II.

Case B - High penetration of wind generation and low offer prices of FFR. The peak wind-power generation in this case is 14391 MW at hour 4 so that the total wind-power penetration is about 50% at that hour. The hourly maximum wind generation profiles are shown in Table V. The capacities of the load resources and their bid and offer prices are the same as Case A.

Case C - High penetration of wind generation and high offer prices of FFR. The wind-power generation in this case is the same as Case B. The capacities of load resources are the same as Case A. We increase the FFR offer price of L2 to \$10/MWh.

TABLE IV. TOTAL HIGH SUSTAINABLE LIMITS OF LOW PENETRATION OF WIND GENERATION

Hour	Wind HSL (MW)						
1	3246	7	2230	13	923	19	2239
2	3587	8	2201	14	611	20	2689
3	3530	9	1764	15	1020	21	2903
4	3598	10	1655	16	1056	22	3177
5	3037	11	1243	17	1454	23	3283
6	2631	12	1261	18	1852	24	3319

TABLE V. TOTAL HIGH SUSTAINABLE LIMITS OF HIGH PENETRATION OF WIND GENERATION

Hour	Wind HSL (MW)						
1	12985	7	11016	13	12870	19	12534
2	14347	8	11526	14	11868	20	11184
3	14121	9	10584	15	11370	21	11610
4	14391	10	11370	16	12036	22	12709
5	12148	11	12078	17	12792	23	13132
6	10524	12	12228	18	13548	24	13275

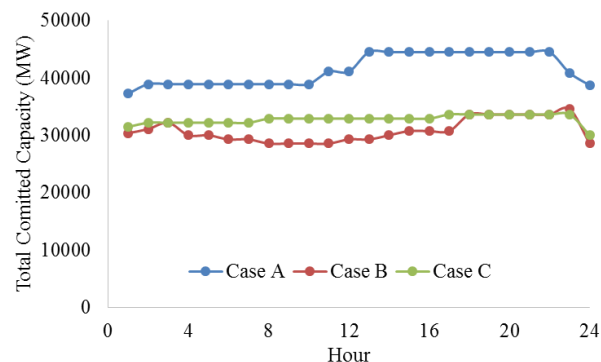


Fig. 5. Total committed capacity of thermal generating units

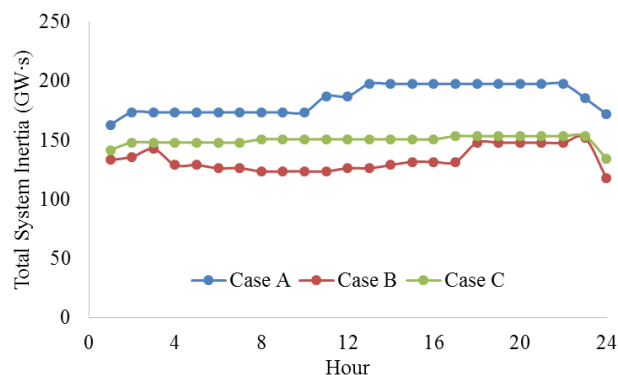


Fig. 6. Total system inertia based on unit commitment

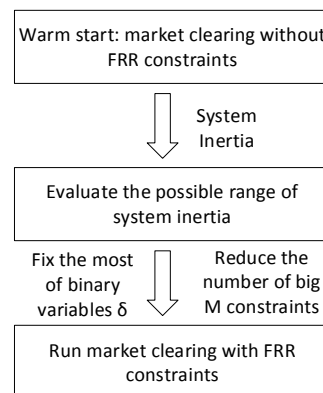


Fig. 7. Proposed warm start process

The social welfare in Case A is \$45,378,657.80 that is lower than that \$50,218,472.72 in Case B and \$50,177,427.09 Case C, respectively, because Case B and Case C have more wind energy scheduled in the next day. Furthermore, load resource L2 has the lower FRR offer price in Case B than that in Case C. As a consequence, the social welfare in Case B is slightly higher than Case C. The wall clock time to solve the problem with and without FRR constraints (29)-(35) are shown in the Table VI. The computational time of the original formulation is longer because of more binary variables and big M constraints. We also propose a warm start process before running the full model of market clearing with FRR constraints. The process is shown in Fig. 7. Basically, the market clearing model is initially executed without FRR constraints. Once it is solved, the system inertia can be calculated accordingly. For those cases when the difference in the total system inertia between with and without considering FRR constraints is expected not to be significant, the most of binary variables δ are fixed except the ones corresponding to the neighboring points in the linearized curve. For example, if the overall system inertia from a warm start execution is 190 GW·s, the binary variables corresponding to the boundary points of its system inertia range, i.e., 177 GW·s and 202 GW·s, will be active – see Table I. Other binary variables are fixed to one or zero. Therefore, the number of binary variables and big M constraints can be reduced significantly. The market clearing model can then be rerun with the proposed FRR constraints to obtain the final solution. The computational time with a warm start is much less than that with the original formulation as listed in Table VI. The social welfare with warm start in Case A, Case B and Case C are \$45,286,559.14, \$50,162,115.60 and \$50,140,493.38 respectively,

TABLE VI. COMPUTATIONAL TIME

Wall clock time (s)		Case A	Case B	Case C
With FRR constraints	Original formulation	7.6	84.6	318.9
	Warm start	9.0	7.8	7.5
Without FRR constraints		4.3	3.2	3.2

The energy bid price of the load resource L3 is very low, so L3 is not awarded and the other two loads are awarded in their full bidding capacities in all three cases. The total hourly committed capacities for the three cases are shown in Fig. 5. Since the wind generation is low in Case A, the total capacity of committed thermal generating units in Case A is the highest among three cases. Case B and Case C have the same cleared wind generation, however, Case C prefers to commit additional units and thus buys PFR from thermal units rather than obtain FFR from LRs. Case C commits more generating capacity to supply the PFR due to the higher FFR offer price of the load resource L2 in Case C.

The total system inertias based on unit commitment for the three cases are given in Fig. 6 in which the trend of the three curves is similar with that in Fig. 5. It is noted that the higher system inertia can result in a lower FRR requirement and a lower PFR/FFR ratio. As a result, the FRR requirement under high wind penetration condition is higher than that under low wind penetration condition. Therefore, more FFR are awarded in Case B than Case A while the cleared PFR are almost the same in the two cases as shown in Fig. 8 and Fig. 9. In Case C, the thermal generating units provide all FRR except the hour 24. The load resource L2 provides additional FFR at hour 24 because all PFR are awarded and committing additional thermal generating units is not economical.

The cleared prices for PFR and FFR are shown in Fig. 10 and Fig. 11. The PFR price is equal to the sum of the dual variables of the constraints (25) and (26). If the thermal generating units are the marginal resources to supply FRR, the PFR price will reflect the PFR offer of those marginal resources such as hour 1-24 in Case C. If the load resources are marginal resources to supply FRR, both PFR offer and FFR offer will impact the PFR cleared price because there is the minimum PFR requirement constraint (25). It is possible that the minimum PFR requirement constraint is binding and the dual variable of (25) is not zero, such as the most hours in Case A and Case B. The cleared FFR price account for the marginal offer of FFR and the equivalency ratio between the FFR and PFR. During hour 1 to hour 23 in Case C, there is no awarded FFR since the cleared FFR price is lower than the FFR offer. In Case A and B, the FFR offer will determine the cleared price of FFR because load resource L2 is the marginal resource to provide FFR.

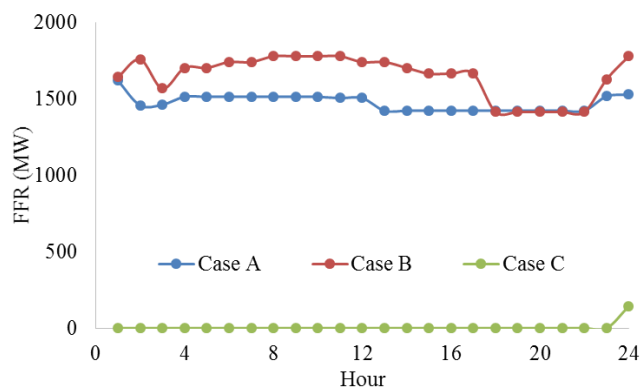


Fig. 8. Cleared FFR in day-ahead market

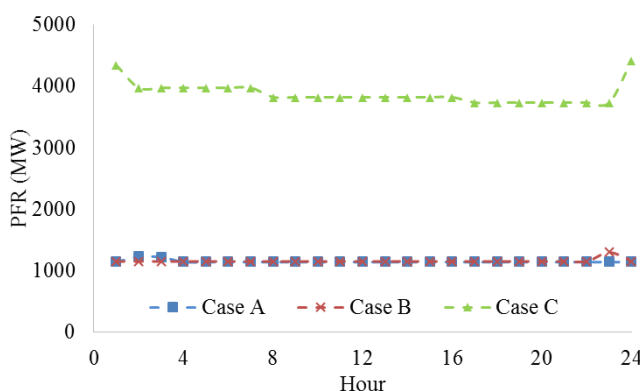


Fig. 9. Cleared PFR in day-ahead market

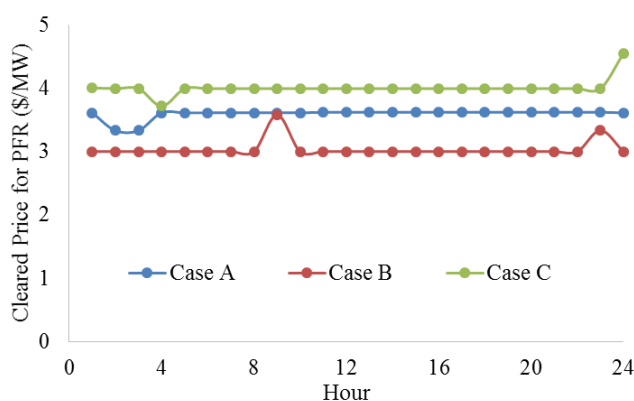


Fig. 10. Cleared price for PFR in day-ahead market

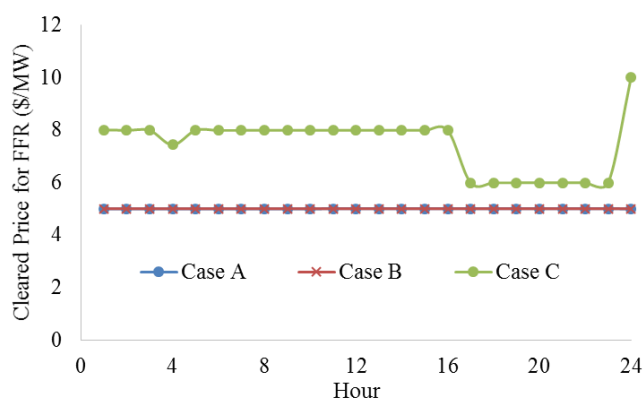


Fig. 11. Cleared price for FFR in day-ahead market

VII. CONCLUSION

This paper discussed how to maintain sufficient PFC capability under high penetration of renewable energy condition. In order to enable both LRs and traditional synchronous generators to offer their PFC capability in the day-ahead market, we propose a day-ahead energy, inertia and reserve co-optimization model. This model includes a constraint to account for the FRR requirement. The equivalency ratio between PFR and FFR, and their dependency on system inertia, which is contributed by committed generating units, is also considered. In this paper, this dependency is approximated as stepwise ratio-inertia curve and piecewise linear FRR requirement-inertia curve. As a result, the co-optimization model includes bilinear terms in the constraints.

A linear reformulation technique with big M is proposed to transform the FRR constraints into linear constraints which can be solved by the commercial solver CPLEX. Three scenarios are simulated to study how the price of PFR/FFR will be formulated under different wind penetration levels. These case studies show the effectiveness of the proposed solution and the correctness of the cleared reserve and prices. Besides, in order to overcome the revenue shortages of generators, uplift payments or the new pricing strategies can be used in the settlement. The proposed formulation and solution methodology in day-ahead market can also be modified and applied into reliability unit commitment.

While this work is primarily focused on the incorporation of LRs in the day-ahead market, the fundamental principle can be extended to other resources which are also able to respond to the large frequency deviations, such as energy storages and synthetic inertia from wind turbines.

ACKNOWLEDGEMENT

The authors are grateful to the assistance from Weifeng Li and Sandip Sharma at ERCOT in preparing this manuscript. The views and opinions of authors expressed in this paper do not necessarily state or reflect those of ERCOT.

REFERENCE

- [1] P. Kundur, *Power System Stability and Control*, McGraw-Hill, 1994.
- [2] Pengwei Du, Y.V. Makarov, M. A. Pai, B. McManus, "Calculating individual resources variability and uncertainty factors based on their contributions to the overall system balancing needs," *IEEE Transactions on Sustainable Energy*, vol. 5, no. 1, Jan. 2014, pp. 323 - 331.
- [3] Pengwei Du, Julia Matevosyan, "Forecast system inertia condition and its impact to integrate more renewables," *IEEE Transactions on Smart Grid*, 2017.
- [4] P. Du, H. Hui, and N. Lu, "Procurement of regulation services for a grid with high-penetration wind generation resources: a case study of ERCOT," *IET Generation, Transmission & Distribution*, 2016, no. 10, vol.16, pp. 4085-4093.
- [5] P. Du, Y. Makarov, "Using disturbance data to monitor primary frequency response for power system interconnections," *IEEE Transactions on Power Systems*, vol. 29, no. 3, May 2014, pp. 1431 - 1432.
- [6] E. Ela, M. Milligan, B. Kirby, A. Tuohy and D. Brooks, "Alternative approaches for incentivizing the frequency responsive reserve ancillary service," NREL, March 2012.
- [7] Eto, Joseph H. "Use of frequency response metrics to assess the planning and operating requirements for reliable integration of variable renewable generation." Lawrence Berkeley National Laboratory (2011).
- [8] NERC Frequency Response Initiative, April, 2010.
- [9] Sandip Sharma, Shun-Hsien Huang and NDR Sarma, "System inertial frequency response estimation and impact of renewable resources in

- ERCOT interconnection,” 2011 IEEE Power and Energy Society General Meeting, pp. 1 - 6, San Diego, CA, 24-29 July, 2011.
- [10] Ronan Doherty, Alan Mullane, Gillian (Lalor) Nolan, Daniel J. Burke, Alexander Bryson, and Mark O'Malley, "An assessment of the impact of wind generation on system frequency control," *IEEE Transactions on Power Systems*, vol. 25, no. 1, pp. 452-460, Feb. 2010.
- [11] O'Sullivan, Jon, et al. "Studying the maximum instantaneous non-synchronous generation in an island system—Frequency stability challenges in Ireland." *IEEE Transactions on Power Systems*, vol.29, no.6, 2014, pp.2943-2951.
- [12] Morren, Johan, et al. "Wind turbines emulating inertia and supporting primary frequency control," *IEEE Transactions on Power Systems*, vol.21, no.1, 2006, pp. 433-434.
- [13] Delille, Uthier, Bruno Francois, and Gilles Malarange. "Dynamic frequency control support by energy storage to reduce the impact of wind and solar generation on isolated power system's inertia," *IEEE Transactions on Sustainable Energy*, vol.3, no.4, 2012, pp.931-939.
- [14] F.D. Galiana, F. Bouffard, J.M. Arroyo, J.F. Restrepo, "Scheduling and pricing of coupled energy and primary, secondary, and tertiary reserves," *Proceedings of the IEEE*, vol. 93, no. 11, pp. 1970–1983, Nov. 2005.
- [15] J.W. O'Sullivan and M.J. O'Malley, "Economic dispatch of a small utility with a frequency based reserve policy," *IEEE Transactions on Power Systems*, vol. 11, no. 3, pp. 1648-1653, August 1996.
- [16] J.W. O'Sullivan, M.J. O'Malley, "A new methodology for the provision of reserve in an isolated power system," *IEEE Transactions on Power Systems*, vol. 14, No. 2, pp. 519-524, May 1999.
- [17] K. A. Papadogiannis and N. D. Hatziaargyriou, "Optimal allocation of primary reserve services in energy markets," *IEEE Transactions on Power Systems*, vol. 19, no. 1, pp. 652-659, Feb. 2004.
- [18] R. Doherty, G. Lalor, M. O'Malley, "Frequency control in competitive electricity market dispatch," *IEEE Transactions on Power Systems*, vol. 20, no. 3, pp. 1588 – 1596, Aug. 2005.
- [19] Erik Ela, Vahan Gevorgian, Aidan Tuohy, Brendan Kirby, Michael Milligan, and Mark O'Malley, "Market designs for the primary frequency response ancillary service—Part I: motivation and design," *IEEE Transactions on Power Systems*, vol. 29, no. 1, pp. 421 – 431, Jan. 2014.
- [20] Erik Ela, Vahan Gevorgian, Aidan Tuohy, Brendan Kirby, Michael Milligan, and Mark O'Malley, "Market designs for the primary frequency response ancillary service—part II: case studies," *IEEE Transactions on Power Systems*, vol. 29, no. 1, pp. 432 – 440, Jan. 2014.
- [21] J.F. Restrepo, F.D. Galiana, "Unit commitment with primary frequency regulation constraints," *IEEE Transactions on Power Systems*, vol. 20, no. 4, pp. 1836 - 1842, Nov. 2005.
- [22] W. Li, P. Du, N. Lu, "Design of a new primary frequency control market for hosting frequency response reserve offers from both generators and loads," *IEEE Transactions on Smart Grid*, 2017 Feb 23.
- [23] C. Liu, A. Botterud, Z. Zhou, and P. Du, "Fuzzy energy and reserve co-optimization with high penetration of renewable energy," *IEEE Transactions on Sustainable Energy*, Vol. 8, no 2, pp. 782-191, 2017.
- [24] Wood, A.J., and B.F. Wollenberg, *Power Generation, Operation and Control*, 2nd Edition, John Wiley & Sons, Inc., New York, NY, 1996.
- [25] Shahidehpour, M., H. Yamin, and Z. Li, *Market Operations in Electric Power Systems*, John Wiley & Sons, Inc., New York, NY, 2002.
- [26] C. Liu, M. Shahidehpour, Z. Li, and M. Fotuhi-Firuzabad "Component & Mode Models for Short-term Scheduling of Combined-cycle Units," *IEEE Trans. Power Syst.*, Vol. 24, pp. 976–990, May 2009.
- [27] C. Lee, C. Liu, S. Mehrotra and M. Shahidehpour, "Modeling Transmission Line Constraints in Two-Stage Robust Unit Commitment Problem," *IEEE Transactions on Power Systems*, vol. 29, no. 3, pp. 1221 - 1231, 2014.
- [28] Y. T. Tan and D.I.S. Kirschen, "Co-optimization of energy and reserve in electricity markets with demand-side participation in reserve services." Power Systems Conference and Exposition, 2006. PSCE'06. 2006 IEEE PES. IEEE, 2006.
- [29] Rajan, D., and S. Takriti, "Minimum Up/Down Polytopes of the Unit Commitment Problem with Start-up Costs," *IBM Research Report*, June 2005.
- [30] NERC Reliability Standard BAL-003 Frequency Response and Frequency Bias Setting, NERC.
- [31] Bhana, Rajesh, and Thomas J. Overbye. "The Commitment of Interruptible Load to Ensure Adequate System Primary Frequency Response," *IEEE Transactions on Power Systems*, vol.31, no. 3, 2016, pp. 2055-2063.
- [32] ERCOT, "Methodology for Determining Minimum Ancillary Service Requirements," [Online].Available: http://www.ercot.com/content/wcm/key_documents_lists/89135/ERCOT_Methodology_for_Determining_Ancillary_Service_Requirements.zip
- [33] ERCOT, Generator Interconnection Status Report, 2017, [Online].Available: <http://www.ercot.com/gridinfo/resource>
- [34] Independent Market Monitor for ERCOT, 2016 State of The Market Report, May 2017.
- [35] L. Fan, J. Wang, R. Jiang, Y. Guan, "Min-max regret bidding strategy for thermal generator considering price uncertainty," *IEEE Transactions on Power Systems*. Vol. 29, No. 5, pp. 2169-2179, 2014.
- [36] Dane A. Schiro, Tongxin Zheng, Feng Zhao, and Eugene Litvinov, "Convex Hull Pricing," FERC technical conference, June 22-24, 2015, Washington, DC.

Cong Liu (S'08, M'10, SM'16) received his B.S. and M.S. degrees in Electrical Engineering from Xi'an Jiaotong University, China, in 2003 and 2006, respectively. He received his Ph.D. degree at the Illinois Institute of Technology in Chicago in 2010. He was a computational engineer-energy systems in the Energy Systems Division of Argonne National Laboratory. Currently, he is working at Electric Reliability Council of Texas (ERCOT) as a senior market operations engineer. His research interests include the electricity market, operation, control and optimization of power systems

Pengwei Du (M'06-SM'12) received Ph.D. degree in electric power engineering from Rensselaer Polytechnic Institute, Troy, New York. Currently, Dr. Du is with the Electric Reliability Council of Texas (ERCOT). Prior to this, he was a senior research engineer with Pacific Northwest National Laboratory (PNNL) of the Department of Energy (DOE). Dr. Du is the recipient of IEEE PES Power System Dynamic Performance Committee Best Paper Prize in 2016 and an editor of IET Generation Transmission & Distribution and IEEE Transactions on Power Systems.